

**Vibration reduction evaluation of a linear system with  
a nonlinear energy sink under a harmonic  
and random excitation\***

Jiren XUE<sup>1</sup>, Yewei ZHANG<sup>1,2,†</sup>, Hu DING<sup>1</sup>, Liqun CHEN<sup>1</sup>

1. Shanghai Institute of Applied Mathematics and Mechanics, Shanghai Key  
Laboratory of Mechanics in Energy Engineering, School of Mechanics and  
Engineering Science, Shanghai University,  
Shanghai 200072, China;

2. Faculty of Aerospace Engineering, Shenyang Aerospace University,  
Shenyang 110136, China

(Received Jun. 25, 2019 / Revised Aug. 20, 2019)

**Abstract** The nonlinear behaviors and vibration reduction of a linear system with a nonlinear energy sink (NES) are investigated. The linear system is excited by a harmonic and random base excitation, consisting of a mass block, a linear spring, and a linear viscous damper. The NES is composed of a mass block, a linear viscous damper, and a spring with ideal cubic nonlinear stiffness. Based on the generalized harmonic function method, the steady-state Fokker-Planck-Kolmogorov equation is presented to reveal the response of the system. The path integral method based on the Gauss-Legendre polynomial is used to achieve the numerical solutions. The performance of vibration reduction is evaluated by the displacement and velocity transition probability densities, the transmissibility transition probability density, and the percentage of the energy absorption transition probability density of the linear oscillator. The sensitivity of the parameters is analyzed for varying the nonlinear stiffness coefficient and the damper ratio. The investigation illustrates that a linear system with NES can also realize great vibration reduction under harmonic and random base excitations and random bifurcation may appear under different parameters, which will affect the stability of the system.

**Key words** nonlinear energy sink (NES), Gauss-Legendre polynomial, transmissibility, percentage of energy absorption

**Chinese Library Classification** O322

**2010 Mathematics Subject Classification** 34A34, 74K30

---

\* Citation: XUE, J. R., ZHANG, Y. W., DING, H., and CHEN, L. Q. Vibration reduction evaluation of a linear system with a nonlinear energy sink under a harmonic and random excitation. *Applied Mathematics and Mechanics (English Edition)*, **41**(1), 1–14 (2020) <https://doi.org/10.1007/s10483-020-2560-6>

† Corresponding author, E-mail: zhangyewei1218@126.com

Project supported by the National Natural Science Foundation of China (Nos.11772205 and 11572182) and the Liaoning Revitalization Talents Program of China (No. XLYC1807172)

©Shanghai University and Springer-Verlag GmbH Germany, part of Springer Nature 2020

## 1 Introduction

Malatkar and Nayfeh<sup>[1]</sup> first proposed that adding nonlinearity to a traditional linear vibration reduction device could effectively increase the bandwidth of the vibration suppression and improve the robustness of the vibration reduction system. Recently, the principle of targeted energy transfer has been prospering as a method of research to achieve the energy transfer from a linear oscillator to a nonlinear oscillator, i.e., the nonlinear energy sink (NES). It is a representative passive vibration reduction device, which is able to achieve the targeted energy transfer. The NES is an effective device to reduce vibration passively<sup>[2-3]</sup>.

In the past years, the steady-state response of multi-degree-of-freedom systems under harmonic excitations has been predicted by numerical simulation methods<sup>[4-10]</sup> and approximate analytical methods<sup>[4,11-15]</sup>, e.g., the complexification averaging method<sup>[4,6,8,11,13-18]</sup> and the harmonic balance method<sup>[19-22]</sup>.

Currently, the vibration reduction efficiency of the linear system coupled with an NES system under complex external excitations is a hot research topic for scholars at home and abroad. Gendelman et al.<sup>[23]</sup> investigated the dynamic response of a small mass with a nonlinear damper under impact loading. Kerschen et al.<sup>[24-25]</sup> studied the vibration reduction mechanism of a two-degree-of-freedom system with an NES. Tsakirtzi et al.<sup>[26]</sup> investigated the dynamic behavior of the multi-degree-of-freedom system coupled with an NES. Shiroky and Gendelman<sup>[27]</sup> investigated the dynamic behavior of a single degree-of-freedom system with an NES under parametric excitations. Starosvetsky and Gendelman<sup>[28]</sup> verified the vibration reduction effect of a single degree-of-freedom system coupled with an NES under narrow-band random excitations with a numerical method. Xiong et al.<sup>[29]</sup> simply sketched out the response regimes of a single degree-of-freedom system coupled with an NES under a narrow-band random excitation. Huang et al.<sup>[30]</sup> analyzed the steady-state response, random jump, and bifurcation phenomenon of the Duffing system under harmonic and white noise excitations. Yan et al.<sup>[31]</sup> studied the dynamic behavior of an axially moving beam excited by harmonic and parametric excitations with the Galerkin truncation method. Zhao et al.<sup>[32]</sup> studied the vehicle random vibration with the pseudo-excitation method. Su et al.<sup>[33]</sup> used the explicit time-domain method to analyze a coupled vehicle-bridge system.

However, the excitations in the aforementioned studies are the most common random ones, and no efficiency of vibration reduction under the excitations has been interpreted sufficiently and intuitively. In view of the above problems, in this paper, the nonlinear behaviors and vibration reduction of a linear system with an NES are investigated. The paper is arranged as follows. In Section 2, a simple model of a linear system with an NES is presented, and the steady-state Fokker-Planck-Kolmogorov equation is determined by the method of generalized harmonic function. In Section 3, the path integral method based on the Gauss-Legendre polynomial is used to calculate the numerical solutions of the steady-state Fokker-Planck-Kolmogorov equation. In Section 4, the responses and evaluation of vibration reduction are simulated under some given parameters. In Section 5, the nonlinear stiffness coefficient and damper ratio are proven to have a significant effect on the vibration reduction. At last, in Section 6, the main conclusions are summarized.

## 2 A linear single degree-of-freedom system coupled with an NES

Consider a linear system with an NES under a harmonic and random excitation (see Fig. 1). The model consists of a mass block  $m_1$ , a linear stiffness  $k_1$ , and a linear viscous damper  $c_1$ . The harmonic and random excitation is  $u(t) = A_u \sin(\omega t) + W(t)$ . The NES is composed of a mass block  $m_2$ , a spring with an ideal cubic nonlinear stiffness  $k_2$ , and a linear viscous damper  $c_2$ .

The model moves in the horizontal direction, and the effects of gravity and friction are

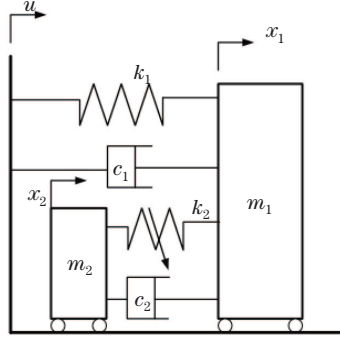


**Fig. 1** A single degree-of-freedom system coupled with an NES

neglected. According to the second Newton's law, the governing dynamic equations are as follows:

$$\begin{cases} m_1 \ddot{x}_1 + c_1 \dot{x}_1 + k_1 x_1 + c_2 (\dot{x}_1 - \dot{x}_2) + k_2 (x_1 - x_2)^3 = c_1 \dot{u} + k_1 u, \\ m_2 \ddot{x}_2 + c_2 (\dot{x}_2 - \dot{x}_1) + k_2 (x_2 - x_1)^3 = 0, \end{cases} \quad (1)$$

where  $x_1$  and  $x_2$  are the displacements of the mass blocks  $m_1$  and  $m_2$ , respectively.

The dimensionless form of Eq. (1) can be obtained as follows:

$$\begin{cases} \ddot{y}_1 + \zeta_1 \dot{y}_1 + y_1 + \zeta_2 (\dot{y}_1 - \dot{y}_2) + \beta (y_1 - y_2)^3 = f_t \sin(\gamma \tau) + \xi(t), \\ \varepsilon \ddot{y}_2 + \zeta_2 (\dot{y}_2 - \dot{y}_1) + \beta (y_2 - y_1)^3 = 0, \end{cases} \quad (2)$$

where  $y_1$  is the dimensionless displacement of the mass block  $m_1$ ,  $y_2$  is the dimensionless displacement of the mass block  $m_2$ ,  $\tau$  is the dimensionless time, and

$$y_1 = \frac{x_1}{l}, \quad y_2 = \frac{x_2}{l}, \quad u_0 = \frac{u}{l}, \quad \tau = \omega_0 t. \quad (3)$$

In the above equations,  $u_0$  is the dimensionless displacement of the base,  $l$  represents the elongation or compression when the linear spring is subjected to an external force of 1 kN. The natural frequency of the linear oscillator  $\omega_0$ , the mass ratio  $\varepsilon$ , the damper ratios of the linear oscillator  $\zeta_1$  and the NES oscillator  $\zeta_2$ , the ideal cubic nonlinear stiffness  $\beta$ , the amplitude of the harmonic excitation  $f_t$ , and the frequency ratio  $\gamma$  are expressed as follows:

$$\begin{cases} \omega_0 = \sqrt{\frac{k_1}{m_1}}, \quad \varepsilon = \frac{m_2}{m_1}, \quad \zeta_1 = \frac{c_1}{m_2 \omega_0}, \\ \zeta_2 = \frac{c_2}{m_2 \omega_0}, \quad \beta = \frac{k_2 l^2}{m_1 \omega_0^2}, \quad f_t = \frac{A_u}{k_1 l}, \quad \gamma = \frac{\omega}{\omega_0}. \end{cases} \quad (4)$$

The random excitation is concretized with the Gaussian white noise, whose strength is two-dimensional, and the autocorrelation function is  $E(\xi(t)\xi(t+\tau)) = \delta(\tau)$  in which  $\delta(\tau)$  is the Dirac delta function.

Some new state variables are introduced as follows:

$$q_1 = y_1, \quad q_2 = y_1 - y_2, \quad p_1 = \dot{q}_1, \quad p_2 = \dot{q}_2. \quad (5)$$

Substitute Eq. (5) into Eq. (2). Then, after applying a few simple algebraic transformations, we can convert Eq. (2) into the following state-space equation:

$$\dot{p}_i + g_i(q_i) = -\varepsilon h_i(p_i; q_i) + \xi(t). \quad (6)$$

Based on the generalized harmonic function method, the solution to Eq. (6) can be assumed to be as follows:

$$q_i(t) = A_i(t) \cos \phi_i(t), \quad p_i(t) = -A_i(t) v_i(A_i, \phi_i) \sin \phi_i(t), \quad \phi_i(t) = \alpha_i(t) + \psi_i(t), \quad (7)$$

where  $v_i = (A_i, \phi_i)$  is the instantaneous angular frequency of the  $i$ th oscillator. It converts a function of the generalized displacement and velocity into a function of magnitude and phase as follows:

$$v_i(A_i, \phi_i) = \frac{d\alpha_i}{dt} = \sqrt{\frac{2(U_i(A_i) - U_i(A_i \cos \phi_i))}{A_i^2 \sin^2 \phi_i}}. \quad (8)$$

Substitute Eq. (7) into Eq. (6). Then, we can obtain the standard random Itô differential equation as follows:

$$\begin{cases} \frac{dA_1}{dt} = F_{11}(A_1, \phi_1, \omega t) + H_{11}\xi(t), & \frac{dA_2}{dt} = F_{21}(A_2, \phi_2, \omega t) + H_{21}\xi(t), \\ \frac{d\phi_1}{dt} = F_{12}(A_1, \phi_1, \omega t) + H_{12}\xi(t), & \frac{d\phi_2}{dt} = F_{22}(A_2, \phi_2, \omega t) + H_{22}\xi(t), \end{cases} \quad (9)$$

where

$$\begin{cases} F_{11} = -\frac{\varepsilon A_1}{g_1(A_1)} h_1 v_1 \sin \phi_1, & H_{11} = -\frac{A_1}{g_1(A_1)} v_1 \sin \phi_1, \\ F_{21} = -\frac{\varepsilon A_2}{g_2(A_2)} h_2 v_2 \sin \phi_2, & H_{21} = -\frac{A_2}{g_2(A_2)} v_2 \sin \phi_2, \\ F_{12} = -\frac{\varepsilon}{g_1(A_1)} h_1 v_1 \cos \phi_1, & H_{12} = -\frac{1}{g_1(A_1)} v_1 \cos \phi_1, \\ F_{22} = -\frac{\varepsilon}{g_2(A_2)} h_2 v_2 \cos \phi_2, & H_{22} = -\frac{1}{g_2(A_2)} v_2 \cos \phi_2. \end{cases} \quad (10)$$

According to the Itô differential law, since the amplitude  $A_i$  is the slow variable and the phase  $\phi_i$  is the fast variable, if the phases are averaged over time, we can denote the deterministic random average Itô differential equation for amplitude and phase difference as follows:

$$\begin{cases} dA_1 = \bar{m}_{11}(A_1, A_2, \Theta)dt + \bar{\sigma}_{11}dB(t), \\ dA_2 = \bar{m}_{21}(A_1, A_2, \Theta)dt + \bar{\sigma}_{21}dB(t), \\ d\Theta = \bar{m}_{12}(A_1, A_2, \Theta)dt + \bar{\sigma}_{12}dB(t), \end{cases} \quad (11)$$

where  $\bar{m}_{11}$ ,  $\bar{m}_{21}$ , and  $\bar{m}_{12}$  are drift coefficients, and  $\bar{\sigma}_{11}$ ,  $\bar{\sigma}_{21}$ , and  $\bar{\sigma}_{12}$  are diffusion coefficients.  $B(t)$  is a standard Wiener process.

The phase difference can be expressed as follows:

$$\Theta = \varepsilon \sigma \tau_1 - \phi_1. \quad (12)$$

The averaged drift coefficients can be expressed as follows:

$$\begin{cases} \bar{m}_{11} = F_{11} + D \left( H_{11} \frac{\partial H_{11}}{\partial A_1} + H_{12} \frac{\partial H_{11}}{\partial \phi_1} \right), \\ \bar{m}_{21} = F_{21} + D \left( H_{21} \frac{\partial H_{21}}{\partial A_2} + H_{22} \frac{\partial H_{21}}{\partial \phi_2} \right), \\ \bar{m}_{12} = F_{12} + D \left( H_{11} \frac{\partial H_{12}}{\partial A_1} + H_{12} \frac{\partial H_{12}}{\partial \phi_1} \right). \end{cases} \quad (13)$$

The averaged diffusion coefficients can be expressed as follows:

$$\begin{cases} \bar{b}_{111} = 2DH_{11}^2, \\ \bar{b}_{211} = 2DH_{21}^2, \\ \bar{b}_{112} = 2DH_{11}H_{12}, \\ \bar{b}_{122} = 2DH_{12}^2. \end{cases}$$

According to Eq. (11), the steady-state Fokker-Planck-Kolmogorov equation can be established as follows:

$$\begin{aligned} \frac{\partial p}{\partial t} = & - \frac{\partial(\bar{m}_{11}p)}{\partial A_1} - \frac{\partial(\bar{m}_{21}p)}{\partial A_2} - \frac{\partial(\bar{m}_{12}p)}{\partial \Theta} \\ & + \frac{1}{2} \frac{\partial^2(\bar{b}_{111}p)}{\partial A_1^2} + \frac{1}{2} \frac{\partial^2(\bar{b}_{211}p)}{\partial A_2^2} + \frac{1}{2} \frac{\partial^2(\bar{b}_{122}p)}{\partial \Theta^2} = 0, \end{aligned} \quad (14)$$

where  $A_1$ ,  $A_2$ , and  $\Theta$  constitute a three-dimensional (3D) state vector  $X(t)$ ,  $m_{11}$ ,  $m_{21}$ , and  $m_{12}$  are 3D averaged drift coefficient function vectors, and  $b_{111}$ ,  $b_{211}$ , and  $b_{122}$  are averaged diffusion coefficient matrix functions.

### 3 Solving the steady-state Fokker-Planck-Kolmogorov equation

It is known that for the general linear systems and some specific single degree-of-freedom nonlinear systems, e.g., the Duffing system and the Van der Pol system, it is easy to get the exact stationary solutions to a transition probability density function; but for complex multi-degree-of-freedom nonlinear systems, it is difficult to get the exact stationary solutions. The transition probability density function can be used to indicate the probability of a stochastic variable appearing at a certain time after a period of time. In terms of vibration reduction, if the transition probability density of the system at the equilibrium position is larger, the performance of vibration reduction will be better. The approximate numerical solution to a transition probability density function can only be obtained by a numerical method, e.g., the finite difference method<sup>[34]</sup>, the cell mapping method<sup>[37]</sup>, and the finite element method<sup>[35–36]</sup>. In this paper, a new revised path integral method is adopted to calculate the numerical solution to the steady-state Fokker-Planck-Kolmogorov equation of our proposed system.

The revised path integral method replaces some complex interpolation integral functions with some discrete Gaussian integration points, and enhances the computational efficiency in solving the high-dimensional high-order partial differential equations without boundary singularity.

In a Markov process, the following equation, called the transition probability density function, can be used to describe the probability of the stochastic variables passing a period of time

s at the moment  $t$ :

$$P(X(t+s) = j | X(t) = i) = P_{ij}(t, t+s). \quad (15)$$

Then, Eq. (14) can be rewritten as follows:

$$\begin{aligned} & \frac{\partial p(X, t | X^0, t_0)}{\partial t} \\ = & - \frac{\partial(\bar{m}_{ij}(X, t | X^0, t_0)p(X, t | X^0, t_0))}{\partial x_i} + \frac{1}{2} \frac{\partial(\bar{b}_{ijk}(X, t | X^0, t_0)p(X, t | X^0, t_0))}{\partial x_i \partial x_j}. \end{aligned} \quad (16)$$

Given an initial probability condition and some appropriate boundary conditions as follows:

$$\lim_{t \rightarrow 0} p(X, t | X^0, t_0) = \delta(X - X^0), \quad (17)$$

$$p(X_i, t) \rightarrow 0 \quad \text{as} \quad \{X\} \rightarrow \pm\infty, \quad (18)$$

the transition probability density function can be used to completely define the statistical steady-state solution.

According to the initial probability condition and the appropriate boundary conditions, the solution to the transition probability density function can be expressed as follows:

$$p(X, t) = \int_{\Omega} p(X, t | X^0, t_0) p(X^0, t_0) dX, \quad (19)$$

where  $\Omega$  is the range of the state vector for  $X(t)$ . The interval  $[t_0, t]$  is divided into  $M$  sub-intervals, and the probability density function can be derived as follows:

$$\begin{aligned} p(X, t) = & \int_{\Omega} p(X, t | X^{M-1}, t_{M-1}) dX^{M-1} \times \int_{\Omega} p(X^{M-1}, t_{M-1} | X^{M-2}, t_{M-2}) dX^{M-2} \times \dots \\ & \times \int_{\Omega} p(X^2, t_2 | X^1, t_1) dX^1 \times \int_{\Omega} p(X^1, t_1 | X^0, t_0) dX^0. \end{aligned} \quad (20)$$

The integral equation (20) can be discretized at Gauss-Legendre orthogonal points and embodied as follows:

$$p(x^i, t_i) = \sum_{k=1}^K \frac{z_k}{2} \sum_{l=1}^L c_{kl} p(x_{kl}^{(i-1)}, t_{i-1}) p(x^i, t_i | x_{kl}^{(i-1)}, t_{i-1}), \quad (21)$$

where  $K$  is the quantity of the sub-intervals,  $L$  is the quantity of the Gauss-Legendre orthogonal points in sub-intervals,  $z_k$  is the length of the sub-intervals, each  $x_{kl}$  is a location of a Gauss-Legendre orthogonal point, and  $c_{kl}$  is the corresponding weight coefficient. According to the initial conditions and boundary conditions, Eq. (21) can be used to calculate the transition probability density function of some point in a certain time point. Given some point in a previous time point, it is convenient to calculate some point in a next time point. However, only the following transition probability density function at the Gauss-Legendre orthogonal points is essential:

$$p(x_{mn}^i, t_i) = \sum_{k=1}^K \frac{z_k}{2} \sum_{l=1}^L c_{kl} p(x_{kl}^{(i-1)}, t_{i-1}) p(x_{mn}^i, t_i | x_{kl}^{(i-1)}, t_{i-1}), \quad (22)$$

where  $m = 1, 2, \dots, K$ , and  $n = 1, 2, \dots, L$ .

It is worth observing that it is generally assumed that the short-term probability density function is approximately Gaussian, but the approximation of the short-term transition probability density function is different at any Gauss-Legendre orthogonal points. Sun and Hsu<sup>[38]</sup> proposed to use the moment equations to derive the first moment and the second moment of the short-term transition probability density function. This method does not require a step size. However, the moment equations of nonlinear stochastic systems are usually infinite and non-closed. Based on the Gaussian truncation method, the short-term displacement and velocity transition probability density functions of the linear and NES oscillators and their joint transition probability density functions can be presented as follows:

$$p(x_{mn}^i, t_i | x_{kl}^{i-1}, t_{i-1}) = \frac{1}{\sqrt{2\pi}\sigma(t_i)} \exp\left(-\frac{(x_{mn}^i - m_1(t_i))^2}{2\sigma^2(t_i)}\right), \quad (23)$$

$$\begin{aligned} & p(x_{mn}^i, y_{mn}^i | x_{kl}^{i-1}, y_{kl}^{i-1}, t_{i-1}) \\ &= \frac{1}{\sqrt{2\pi}\sigma_1(t_i)\sigma_2(t_i)\sqrt{1-\rho_{12}(t_i)}} \exp(-((\sigma_2^2(t_i)(x_{mn}^i - m_{10}(t_i))^2 \\ & \quad - 2\sigma_1(t_i)\sigma_2(t_i)(x_{mn}^i - m_{10}(t_i))(y_{mn}^i - m_{01}(t_i)) \\ & \quad + \sigma_1^2(t_i)(y_{mn}^i - m_{01}(t_i))^2)(2\sigma_1^2(t_i)\sigma_2^2(t_i)(1-\rho_{12}(t_i))^2)), \end{aligned} \quad (24)$$

where

$$\begin{cases} m_{ij} = E[X^i \dot{X}^j], & \sigma_1^2(t_i) = m_{20}(t_i) - (m_{10}(t_i))^2, \\ \sigma_2^2(t_i) = m_{02}(t_i) - (m_{01}(t_i))^2, & \sigma_1(t_i)\sigma_2(t_i)\rho_{12}(t_i) = m_{11}(t_i) - m_{10}(t_i)m_{01}(t_i). \end{cases} \quad (25)$$

Substitute Eq. (25) into Eqs. (23) and (24). Then, the global transition probability density function can be obtained

#### 4 Simulation

The reduced interval for the path integral method is selected from  $-0.5$  to  $0.5$ , and is divided into 500 consistent sub-intervals with 10 Gauss-Legendre orthogonal points in each sub-interval, i.e.,  $K = 500$ ,  $z_k = 1/500$ , and  $L = 10$ . The time step is 0.01.

In order to better evaluate the performance of the vibration reduction of the system under the harmonic and random excitation, the transmissibility transition probability density defined by the standard deviation ratio of the passed force and the excitation and the percentage of the energy absorption transition probability density of the linear oscillator are used to evaluate the performance of the vibration reduction of the system.

$$T = \frac{S_d(y_1 + \zeta_1 \dot{y}_1)}{D + R_{MS}(f_t \sin(\gamma\tau))}, \quad (26)$$

$$\eta_p = A/B, \quad (27)$$

where

$$\begin{cases} A = S_d\left(\frac{1}{2}m_1\dot{y}_1^2 + \frac{1}{2}\omega_0^2 y_1^2 + \int_0^t c_1 \dot{y}_1^2(t) dt\right), \\ B = S_d\left(\frac{1}{2}m_1\dot{y}_1^2 + \frac{1}{2}\omega_0^2 y_1^2 + \int_0^t c_1 \dot{y}_1^2(t) dt + \frac{1}{2}m_2\dot{y}_2^2 \right. \\ \quad \left. + \frac{1}{2}k_n(y_1 - y_2)^4 + \int_0^t c_1(\dot{y}_1^2(t) - \dot{y}_2^2(t)) dt\right). \end{cases}$$

**Table 1** Parameters and their values

Parameter	Symbol	Value
Nonlinear stiffness coefficient	$k_2$	300
Damper ratio of the linear oscillator	$\zeta_1$	0.1
Damper ratio of the NES oscillator	$\zeta_2$	0.15
Mass ratio	$\varepsilon$	0.1
Harmonic excitation amplitude	$f_t$	10
Frequency ratio	$\gamma$	0.5
Strength of Gaussian white noise	$D$	0.01

Figures 2 and 3 depict the transition probability densities of the displacement and velocity of the linear and the NES oscillators. The numerical result shows that the peak of the linear oscillator coupled with the NES in the equilibrium is higher than the peak of a two-degree-of-freedom linear system.

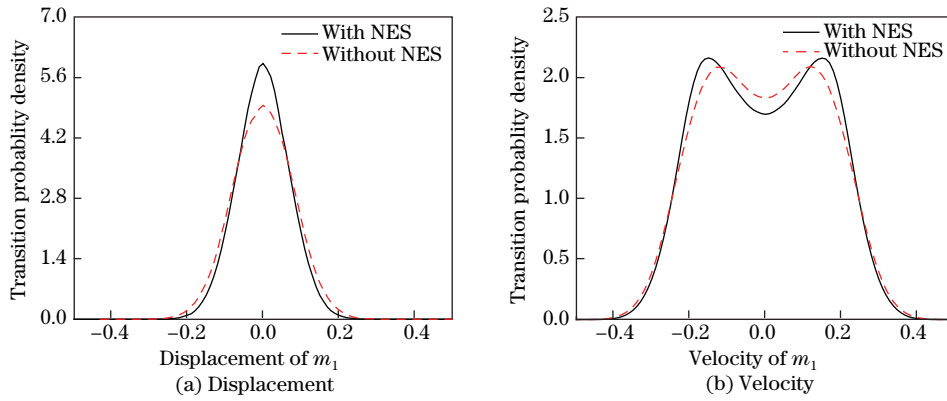
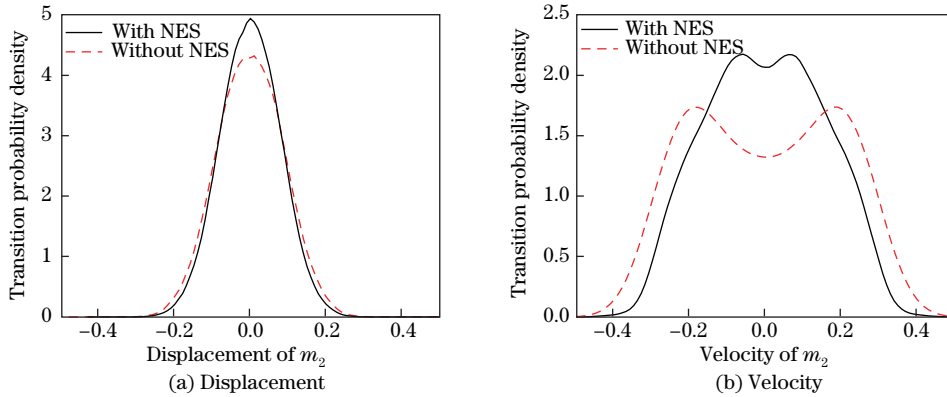
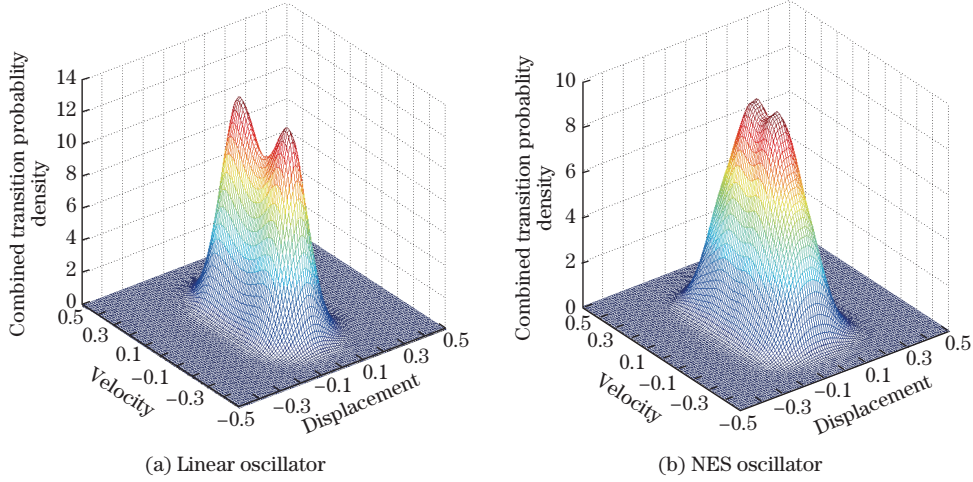
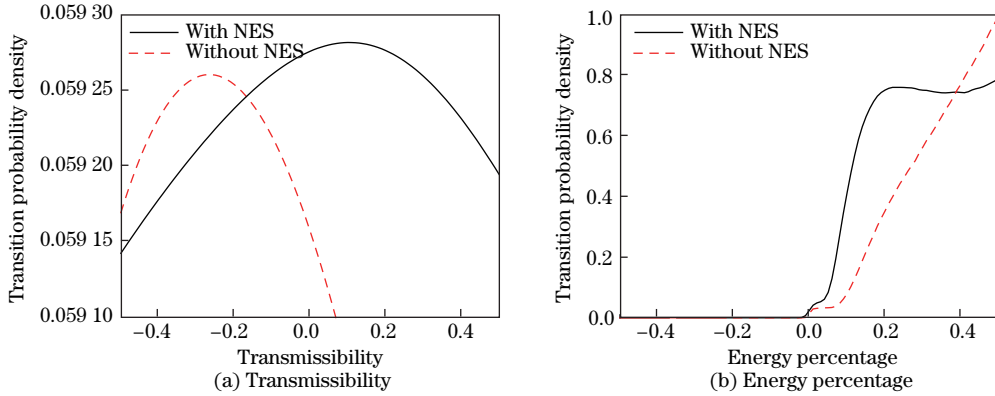
**Fig. 2** Transition probability densities of the displacement and velocity of the linear oscillator**Fig. 3** Transition probability densities of the displacement and velocity of the NES oscillator

Figure 4 shows the joint transition probability densities of the displacement and velocity of the linear and NES oscillators. From Fig. 4, we can see a typical response exhibiting a random jump phenomenon of the linear system coupled with the NES under the joint harmonic and Gaussian white noise. The essence of random jump is a response transition, and is near the equilibrium state.



**Fig. 4** Combined transition probability densities of the displacement and velocity of the linear and NES oscillators (color online)

Figures 5 and 6 reveal the transmissibility transition probability density and the energy absorption percentage of the linear oscillator transition probability density. From the figures, it can be seen that the transition probability density of the linear oscillator coupled with the NES is larger than that of the two-degree-of-freedom linear system when the transmissibility and the energy absorption percentage of the linear oscillator are close to zero.

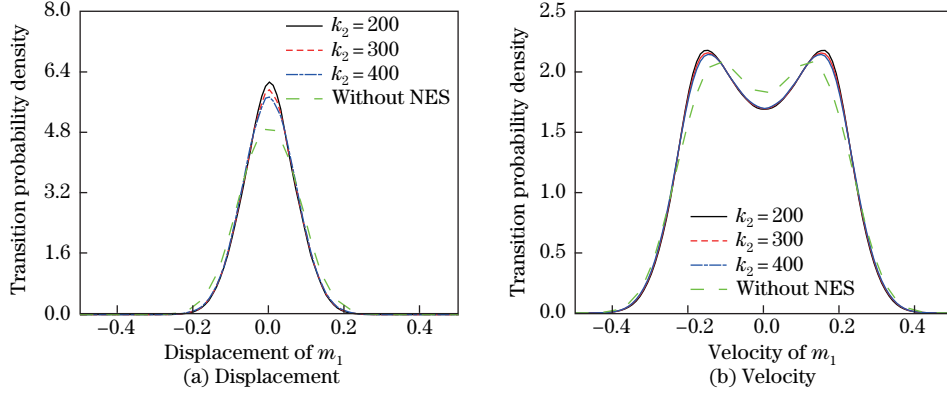


**Fig. 5** Transition probability densities of transmissibility and energy percentage

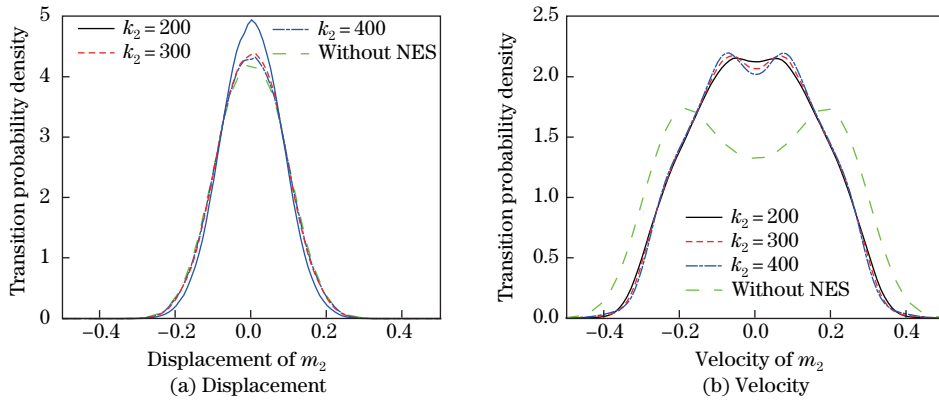
## 5 Parameters analysis

In order to discuss and analyze the effects of the vibration reduction performance of the linear system coupled with the NES under harmonic and Gaussian white noise excitations with different parameters, the effects of the nonlinear stiffness  $k_2$  and the damper ratio  $\zeta_2$  are investigated.

Figures 6 and 7 show the probability densities of the displacement and velocity of the linear and NES oscillators except the difference in the nonlinear stiffness. It can be seen that in all four cases shown in Figs. 6 and 7, the velocity transition probability density is bimodal, which indicates that random jump may occur. However, there is still a slight difference between them. The two peaks are slightly separated, and jump occurs more likely with the increase in the nonlinear stiffness.

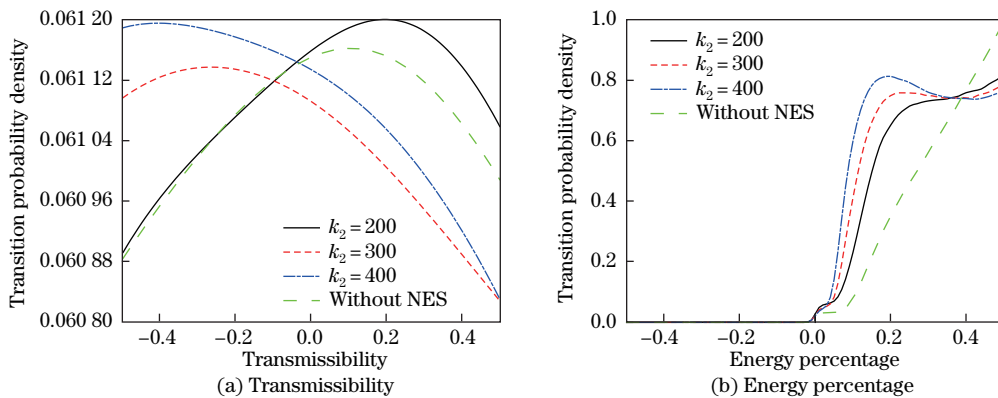


**Fig. 6** Transition probability densities of the displacement and velocity of the linear oscillator except the difference in the nonlinear stiffness



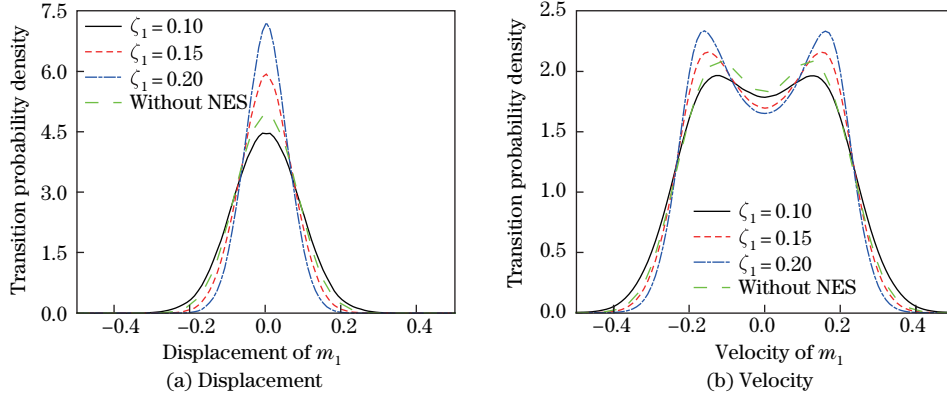
**Fig. 7** Transition probability densities of the displacement and velocity of the NES oscillator except the difference in the nonlinear stiffness

Figure 8 presents the transition probability densities of the transmissibility and energy absorption percentage of the linear oscillator except the difference of the nonlinear stiffness. It can be seen that the transition probability density increases with the increase in the nonlinear stiffness when the transmissibility and the energy absorption percentage of the linear oscillator approaches to zero.



**Fig. 8** Transition probability densities of the transmissibility and energy percentage except the difference in the nonlinear stiffness

Figures 9 and 10 present the probability densities of the displacement and velocity of the linear and NES oscillators except the difference of the damper ratio. In all four cases shown in Figs.9 and 10, the velocity transition probability density is bimodal. Not only it is possible for the occurrence of random jump, but also there is a large difference between them. The two peaks are obviously separated, and jump occurs more likely with the increase in the damper ratio. It can be expected that when the damper ratio approaches to zero, the random jump may disappear. The appearance and disappearance of random jump with the changes of the system parameters are called random jump bifurcations.



**Fig. 9** Transition probability densities of the displacement and velocity of the linear oscillator except the difference in the damper ratio

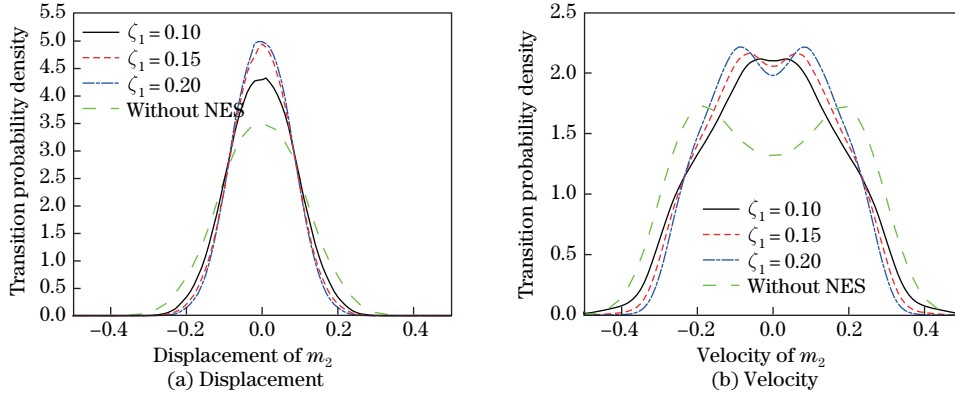


**Fig. 10** Transition probability densities of the displacement and velocity of the NES oscillator except the difference in the damper ratio

Figure 11 presents the transition probability densities of the transmissibility and energy absorption percentage of the linear oscillator except the difference in the damper ratio. The transition probability density decreases with the increase in the damper ratio when the transmissibility or the energy absorption percentage of the linear oscillator is close to zero.

## 6 Conclusions

This paper mainly focuses on the numerical calculation of the response of the linear system with an NES under a harmonic and Gaussian white noise excitation. The path integral based

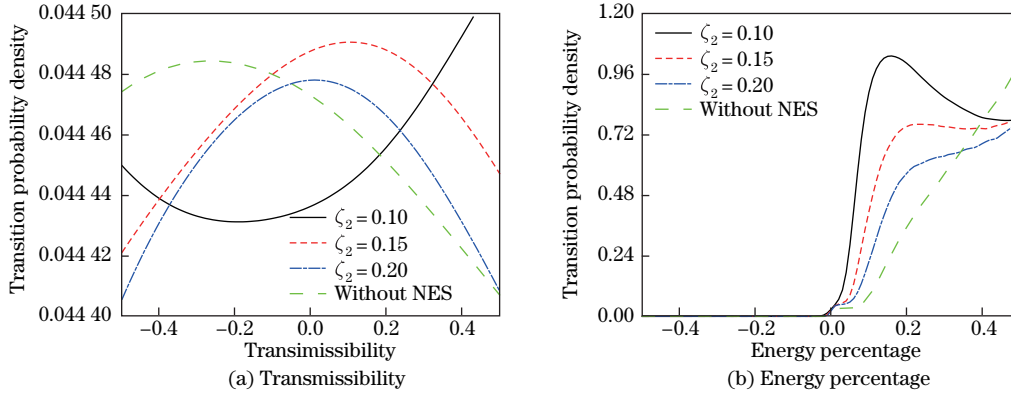


**Fig. 11** Transition probability densities of the transmissibility and energy percentage of the linear oscillator except the difference in the damper ratio

on the Gauss-Legendre polynomial is used to solve the steady-state Fokker-Planck-Kolmogorov equation. The transition probability densities of displacement and velocity are used to determine the dynamical behaviors. The transition probability densities of the transmissibility and input energy absorption percentage of the linear oscillator are used as the indicators to evaluate the performance of vibration reduction. The investigation shows that an NES with reasonable parameters also has an efficient effect of vibration reduction. The conclusions lie in the following aspects.

(i) The linear system with an NES still has a good performance of vibration reduction under a harmonic and random excitation.

(ii) Random jump may appear in the linear system with an NES. The jump may occur from one peak to another peak randomly at any frequency of the harmonic excitation. It is harmful to the stability of the linear system with an NES system.

(iii) Increasing the nonlinear stiffness can effectively improve the vibration reduction performance of the linear system with an NES while ignoring its influence on the system stability, because the change is slight in the same system except the difference in the nonlinear stiffness. Decreasing the damping ratio can effectively improve the performance of vibration reduction of the linear system with an NES and enhance the stability at the same time.

## References

- [1] MALATKAR, P. and NAYFEH, A. F. Steady-state dynamics of a linear structure weakly coupled to an essentially nonlinear oscillator. *Nonlinear Dynamics*, **47**, 167–179 (2006)
- [2] LEE, Y. S., VAKAKIS, A. F., and BERGMAN, L. A. Passive non-linear targeted energy transfer and its application to vibration absorption: a review. *Proceedings of the Institution of Mechanical Engineers, Part J: Journal of Engineering Tribology*, **222**, 77–134 (2008)
- [3] VAKAKIS, A. F., GENDELMAN, O. V., BERGMAN, L. A., MCFARLAND, D. M., KERSCHEN, G., and LEE, Y. S. Nonlinear targeted energy transfer in mechanics and structural systems. *Solid Mechanics and Its Application*, **156**, 88–159 (2009)
- [4] JIANG, X., MCFARLAND, D. M., and BERGMAN, L. A. Steady state passive nonlinear energy pumping in coupled oscillators: theoretical and experimental results. *Nonlinear Dynamics*, **33**, 87–102 (2003)
- [5] SAVADKOOHI, A. T., MANEVITCH, L. I., and LAMARQUE, C. H. Analysis of the transient behavior in a two-degree-of-freedom nonlinear system. *Chaos Solution and Fractals*, **44**, 450–463 (2011)

- 
- [6] SAVADKOOHI, A. T., LAMARQUE, C. H., and DIMITRIJEVIC, Z. Vibratory energy exchange between a linear and a non-smooth system in the presence of the gravity. *Nonlinear Dynamics*, **70**, 1473–1483 (2012)
- [7] WEISS, M., CHENIA, M., and SAVADKOOHI, A. T. Multi-scale energy exchanges between an elasto-plastic oscillator and a light non-smooth system with external pre-stress. *Nonlinear Dynamics*, **83**, 109–135 (2016)
- [8] LAMARQU, C. H., SAVADKOOHI, A. T., and CHARLEMAGNE, S. Nonlinear vibratory interactions between a linear and a non-smooth forced oscillator in the gravitational field. *Mechanical System and Signal Processing*, **89**, 131–148 (2017)
- [9] YANG, K., ZHANG, Y. W., and DING, H. Nonlinear energy sink for whole-spacecraft vibration reduction. *Journal of Vibration and Acoustics*, **139**, 021011 (2017)
- [10] ZANG, J. and CHEN, L. Q. Complex dynamics of a harmonically excited structure coupled with a nonlinear energy sink. *Acta Mechanica Sinica*, **33**, 801–822 (2017)
- [11] GENDELMAN, O. V., STAROSVETSKY, Y., and FELDMAN, M. Attractors of harmonically forced linear oscillator with attached nonlinear energy sink I: description of response regimes. *Nonlinear Dynamics*, **51**, 31–46 (2007)
- [12] STAROSVETSKY, Y. and GENDELMAN, O. V. Attractors of harmonically forced linear oscillator with attached nonlinear energy sink II: optimization of a nonlinear vibration absorber. *Nonlinear Dynamics*, **51**, 47–57 (2007)
- [13] STAROSVETSKY, Y. and GENDELMAN, O. V. Response regimes of linear oscillator coupled to nonlinear energy sink with harmonic forcing and frequency detuning. *Journal of Sound and Vibration*, **315**, 746–765 (2008)
- [14] STAROSVETSKY, Y. and GENDELMAN, O. V. Strongly modulated response in forced 2DOF oscillatory system with essential mass and potential asymmetry. *Physical D: Nonlinear Phenomena*, **237**, 1719–1733 (2008)
- [15] BELLIZZI, S., COTE, R., and PACHEBAT, M. Response of a two-degree-of-freedom system coupled to a nonlinear damper under multi-forcing frequencies. *Journal of Sound and Vibration*, **332**, 1639–1653 (2013)
- [16] PARSEH, M., DARDEL, M., and GHASEMI, M. H. Performance comparison of nonlinear energy sink and linear tuned mass damper in steady-state dynamics of a linear beam. *Nonlinear Dynamics*, **81**, 1981–2002 (2015)
- [17] TAGHIPOUR, J. and DARDEL, M. Steady-state dynamics and robustness of a harmonically excited essentially nonlinear oscillator coupled with a two-DOF nonlinear energy sink. *Mechanical Systems and Signal Processing*, **62-63**, 164–182 (2015)
- [18] YE, S. Q., MAO, X. Y., DING, H., JI, J. C., and CHEN, L. Q. Nonlinear vibrations of a slightly curved beam with nonlinear boundary conditions. *International Journal of Mechanical Sciences*, **168**, 105294 (2020)
- [19] MALATKAR, P. and NAYFEH, A. H. Steady-state dynamics of a linear structure weakly coupled to an essentially nonlinear oscillator. *Nonlinear Dynamics*, **47**, 167–179 (2006)
- [20] LI, X., ZHANG, Y. W., and DING, H. Integration of a nonlinear energy sink and a piezoelectric energy harvester. *Applied Mathematics and Mechanics (English Edition)*, **38**(7), 1019–1030 (2017) <https://doi.org/10.1007/s10483-017-2220-6>
- [21] LUONGO, A. and ZULLI, D. Dynamic analysis of externally excited NES-controlled systems via a mixed multiple scale harmonic balance algorithm. *Nonlinear Dynamics*, **70**, 2049–2061 (2012)
- [22] GUO, H. L., CHEN, Y. S., and YANG, T. Z. Limit cycle oscillation suppression of 2-DOF airfoil using nonlinear energy sink. *Applied Mathematics and Mechanics (English Edition)*, **34**(10), 1277–1290 (2013) <https://doi.org/10.1007/s10483-013-1744-7>
- [23] GENDELMAN, O. V., GORLOV, D. V., and MANEVITCH, L. I. Dynamics of coupled linear and essentially nonlinear oscillators with substantially different masses. *Journal of Sound and Vibration*, **286**, 1–19 (2005)

- 
- [24] KERSCHEN, G., KOWTKO, J. J., and MCFARLAND, D. M. Theoretical and experimental study of multimodal targeted transfer in a system of coupled oscillators. *Nonlinear Dynamics*, **47**, 285–309 (2006)
- [25] KERSCHEN, G., MCFARLAND, D. M., and KOWTKO, J. J. Experimental demonstration of transient resonance capture in a system of two coupled oscillators with essential stiffness nonlinearity. *Journal of Sound and Vibration*, **195**, 822–838 (2007)
- [26] TSAKIRTZI, S., KERSCHEN, G., and PANAGOPOULOS, P. N. Multi-frequency nonlinear energy transfer from linear oscillators to mode essentially nonlinear attachments. *Journal of Sound and Vibration*, **285**, 483–490 (2005)
- [27] SHIROKY, I. B. and GENDELMAN, O. V. Essentially nonlinear vibration absorber in a parametrically excited system. *Zeitschrift für Angewandte Mathematik und Mechanik*, **88**, 573–596 (2008)
- [28] STAROSVETSKY, Y. and GENDELMAN, O. V. Response regimes in forced system with nonlinear energy sink: quasi-periodic and random forcing. *Nonlinear Dynamics*, **64**, 177–195 (2011)
- [29] XIONG, H., KONG, X. R., YANG, Z. G., and LIU, Y. Response regimes of narrow-band stochastic excited linear oscillator coupled to nonlinear energy sink. *Chinese Journal of Aeronautics*, **28**, 55–101 (2015)
- [30] HUANG, Z. L., ZHU, W. Q., and SUZUKI, Y. Stochastic averaging of strongly non-linear oscillators under combined harmonic and white noise excitations. *Journal of Sound and Vibration*, **238**, 233–256 (2000)
- [31] DING, H., ZHU, M. H., and CHEN, L. Q. Dynamic stiffness method for free vibration of an axially moving beam with generalized boundary conditions. *Applied Mathematics and Mechanics (English Edition)*, **40**(7), 911–924 (2019) <http://doi.org/10.1007/s10483-019-2493-8>
- [32] ZHAO, Y., ZHANG, Y. H., and LIN, J. H. Summary on the pseudo-excitation method for vehicle random vibration PSD analysis (in Chinese). *Applied Mathematics and Mechanics*, **34**, 34–55 (2013)
- [33] SU, C., ZHONG, C. Y., and ZHOU, L. C. Random vibration analysis of coupled vehicle-bridge systems with the explicit time-domain method (in Chinese). *Applied Mathematics and Mechanics*, **38**, 107–158 (2017)
- [34] WOJTKIEWICZ, S. F., BERGMAN, L. A., and SPENCER JR, B. F. *Robust Numerical Solution of the Fokker-Planck-Kolmogorov Equation for Two Dimensional Stochastic Dynamical Systems*, Technical Report AAE 94-08, Department of Aeronautical and Astronautica Engineering, University of Illinois at Urbana-Champaign, Urbana-Champaign (1994)
- [35] LANGLEY, R. S. A finite element method for the statistics of non-linear random vibration. *Journal of Sound and Vibration*, **101**, 41–54 (1985)
- [36] KUMAR, P. and NARAYANAN, S. Solution of Fokker-Planck equation by finite element and finite difference methods for nonlinear system. *SADHANA*, **31**, 455–473 (2006)
- [37] KUMAR, M., CHAKRAVORTY, S., and JOHN, J. L. Computational nonlinear stochastic control based on the Fokker-Planck-Kolmogorov equation. *American Institute of Aeronautics and Astronautics*, **25**, 1–15 (2008)
- [38] SUN, J. Q. and HSU, C. S. The generalized cell mapping method in nonlinear random vibration based on short-time Gaussian approximation. *Journal of Applied Mechanics*, **57**, 1018–1025 (1990)